Talanta 105 (2013) 327–332

Contents lists available at SciVerse ScienceDirect

Talanta

journal homepage: www.elsevier.com/locate/talanta

# High performance $H_2$ sensor based on $ZnSnO_3$ cubic crystallites synthesized by a hydrothermal method

Parmeshwar Wadkar, Dipak Bauskar, Pradip Patil *

*Department of Physics, North Maharashtra University, Jalgaon 425001, Maharashtra, India*

ARTICLE INFO

*Article history:*
Received 29 July 2012
Received in revised form
12 October 2012
Accepted 15 October 2012
Available online 23 October 2012

*Keywords:*
$ZnSnO_3$ cubic crystallites
$H_2$ sensor
Semiconductor gas sensors
Hydrothermal method
XRD

ABSTRACT

Zinc stannate ($ZnSnO_3$) cubic crystallites have been successfully synthesized by hydrothermal reaction at 140 °C. X-ray diffraction (XRD), field emission scanning electron microscopy (FESEM) and transmission electron microscopy (TEM) have been employed to characterize the crystal structure and morphology of the as-synthesized $ZnSnO_3$. The $ZnSnO_3$ cubic crystallites exhibited selective sensing performance towards $H_2$ in terms of higher gas response, rapid response-recovery, repeatability and relatively lower operating temperature. This experimental result demonstrates that the synthesized $ZnSnO_3$ cubic crystallites have noteworthy $H_2$ sensing characteristics which make them a promising material for the fabrication of high performance $H_2$ sensor.



## 1. Introduction

In recent years, metal oxide nanostructures including nanoparticles, nanorods, nanotubes, nanowires and nanoribbons have been investigated for gas sensing applications due to some advantageous features such as low cost, simplicity in fabrication, non-toxicity, high gas response, fast response and recovery, selectivity and suitability to different doping [1–3]. The significantly increased surface-to-volume ratio, great level of crystallinity and modified physical/chemical properties of these nanostructures are believed to provide numerous active sites for the interaction with the target gas, which results in excellent gas sensing behavior even at room temperature [2–4]. At the same time, the synthesis method has an effect on the sensor performance largely since it affects the morphology and structure of the sensing material. Various transition metal oxide nanostructures such as $Co_3O_4$ nanorods [5], CdO nanoparticles [6], $\alpha$-$Fe_2O_3$ nanorods [7], $SnO_2$ nanotubes [8], $In_2O_3$ nanowires [9], CuO nanoribbons [10] and ZnO nanorods [11] have been studied as gas sensing materials during the past few years.

$ZnSnO_3$ with various morphologies have been investigated recently as a new type of good gas sensing material [12–16]. However, these gas sensing investigations are limited to ethanol, formaldehyde, butane and $H_2S$. For example, Xu et al. [12] have reported the synthesis of hexagonal shaped $ZnSnO_3$ microparticles via a hydrothermal reaction without any surfactant and investigated their $H_2S$ sensing properties. Xue et al. [13] have synthesized $ZnSnO_3$ nanowires by thermal evaporation method and studied their ethanol sensing properties. Zeng et al. [14] have reported the synthesis of hierarchical $ZnSnO_3$ nanocages via a hexamethylenetetramine (HMT)-assisted hydrothermal reaction and investigated the ethanol sensing properties. Wang et al. [15] have prepared $ZnSnO_3$ cubic crystallites via a solution process at a reaction temperature of 0 °C without any surfactant, which exhibited high sensitivity, fast response and short recovery times towards HCHO gas. The synthesis of $ZnSnO_3$ hollow microspheres by the cetyltrimethyl ammonium bromide (CTAB)-assisted hydrothermal reaction was reported by Fan et al. [16] and they have studied the butane sensing properties.

Hydrogen ($H_2$) is a potential fuel for cars, buses, and other vehicles [17]. It is also already used in medicine and space exploration as well as in the production of industrial chemicals and food products. As it is tasteless, colorless and odorless, it cannot be detected by human beings. It is potentially hazardous due to the high possibility of explosion accidents caused by leakage or by human error. Therefore, hydrogen detection is of great importance during its production, storage and use.

Within the present investigation, experiments have been carried out for the fabrication of a fast responding and selective $H_2$ sensor based on $ZnSnO_3$ cubic crystallites. There is hardly any report on $H_2$ sensor based on $ZnSnO_3$ cubic crystallites. In this study, the $ZnSnO_3$ cubic crystallites were synthesized via a HMT-assisted hydrothermal reaction at 140 °C. Sensing characteristics of the $ZnSnO_3$ cubic crystallites to $H_2$ were systematically investigated. A sensing mechanism was also discussed based on experimental findings.

* Corresponding author. Tel.: +91 257 2257474; fax: +91 257 2258403.
*E-mail addresses:* pppatil@nmu.ac.in, pnmu@yahoo.co.in (P. Patil).

0039-9140/$ - see front matter © 2012 Elsevier B.V. All rights reserved.
http://dx.doi.org/10.1016/j.talanta.2012.10.051

## 2. Experimental

### 2.1. Synthesis of $ZnSnO_3$ cubic crystallites

The synthesis of $ZnSnO_3$ cubic crystallites was carried out using analytical grade zinc acetate ($Zn(CH_3COO)_2 \cdot 2H_2O$), stannic chloride hydrated ($SnCl_4 \cdot 5H_2O$), HMT ($(CH_2)_6N_4$) and sodium hydroxide (NaOH) without further purification. In a typical experiment, 0.2 mmol $Zn(CH_3COO)_2 \cdot 2H_2O$, 0.2 mmol $SnCl_4 \cdot 5H_2O$ and 0.015 mmol $(CH_2)_6N_4$ were dissolved in double distilled water and stirred continuously for 1 h at room temperature (25 °C). An appropriate amount of NaOH was added drop-wise to the reaction mixture with continuous stirring until the final solution pH value of about 10 was achieved. The solution was transferred to a Teflon-lined stainless steel autoclave, maintained at 140 °C for 8 h and then cooled to room temperature naturally. The white colored precipitate was collected by centrifugation, washed several times using double distilled water and ethanol, and then dried in an oven at 100 °C overnight to obtain the end-product for further characterization.

### 2.2. General characterization

The structural analysis of the as-synthesized $ZnSnO_3$ cubic crystallites was carried out using X-ray diffractometer (XRD, D8 Advance, Bruker AXS) with $CuK_\alpha$ radiation ($\lambda = 1.5418$ Å), whereas the surface morphological studies were performed using a field emission scanning electron microscope (FESEM, S-4800, Hitachi, Japan) and a transmission electron microscope (TEM, 1200 EX, JEOL, Japan).

### 2.3. Gas sensing measurements

The $ZnSnO_3$ cubic crystallites powder was pressed into pellets under a pressure of 15 MPa and the ohmic contacts were made with the help of silver paste to form the sensing element. The schematic diagram of the sensing element is shown in Fig. 1. The gas sensing studies were carried out on these sensing elements in a static gas chamber to sense $H_2$ in air ambient. The sensing element was kept directly on a heater in the gas chamber and the temperature was varied from 200 to 400 °C. The temperature of the sensing element was monitored by chromel–alumel thermocouple placed in contact with it. The known volume of the $H_2$ was introduced into the gas chamber pre-filled with air with a micro-syringe so as to yield a desired concentration and it was maintained at atmospheric pressure. The electrical resistance of the sensing element was measured before and after exposure to $H_2$ under a voltage of 5 V using an electrometer (6517B Electrometer, Keithley) controlled by the test software supplied by Biotronic systems, Mumbai, India. The performance of the sensing element is presented in terms of gas response ($S$), which is defined as

$$S = \frac{R_{air}}{R_{gas}} \tag{1}$$

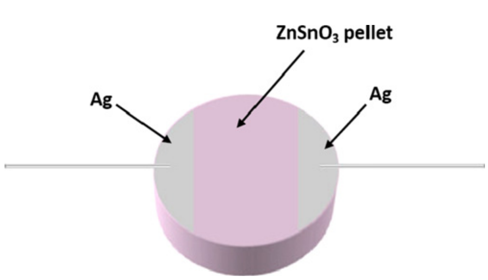


**Fig. 1.** Schematic diagram of the sensor device.

where $R_{air}$ and $R_{gas}$ are the electrical resistance values of the sensor element in air and in the presence of $H_2$ gas, respectively.

## 3. Results and discussion

### 3.1. XRD analysis

The XRD pattern of as-synthesized product is depicted in Fig. 2(a). All of the diffraction peaks can be indexed to the standard $ZnSnO_3$ with the perovskite structure (JCPDS no.: 11-0274), confirming that the as-synthesized product has a typical face centered cubic (FCC) crystal structure. No diffraction peaks due to impurities or other crystalline byproducts such as ZnO or $SnO_2$ were detected, indicating that pure $ZnSnO_3$ crystallites could be obtained under present synthesis conditions.

### 3.2. Morphological studies

Fig. 2(b) shows the FESEM image of the as-synthesized product, which reveals the formation of microcubes with an average edge lengths of about 250–400 nm. Besides, the random aggregation of amorphous nanoparticles is seen on the surface of cubes. The TEM image of the the as-synthesized product is shown in Fig. 2(c). The formation of $ZnSnO_3$ microcubes observed by FESEM previously was confirmed by the TEM. The corresponding selected area electron diffraction (SAED) pattern (as shown in Fig. 2(d)) further confirms that the microcubes have good crystallinity and there is no secondary phase.

### 3.3. Gas sensing performance

In order to determine the optimum operating temperature, the gas response of the $ZnSnO_3$ cubic crystallites based sensor towards 50 ppm $H_2$ was investigated as a function of operating temperature and the corresponding result is shown in Fig. 3. It can be seen that the operating temperature significantly affects the gas response. In general, the change in the operating temperature alters the kinetics of the adsorption and reaction occuring on the sensor surface, which leads to the variation in the gas response. As can be seen from Fig. 3, the gas response continuously increases when the operating temperature varies from 200 to 375 °C and then gradually decreases with a further increase in the operating temperature.

As the progressive adsorption and subsequent surface reactions occur with an increase in the temperature, the gas response of the sensor continuously increases as the temperature increases from 225 to 375 °C. At temperature 375 °C, the optimum balances between the adsorption and desorption, the surface reactions and diffusion length may be established and consequently, the $H_2$ reacts most effectively with chemisorbed oxygen at such particular temperature, which results in the significant decrease in the resistance of the sensor. Therefore, the maximum gas response of the $ZnSnO_3$ cubic crystallites based sensor towards $H_2$ is expected at such particular temperature. At higher temperatures ($>375$ °C), desorption process is dominant and also the diffusion length becomes lower. Therefore, in presence of the $H_2$, the probability of the reduction reaction of the gas with chemisorbed oxygen is less, which results into a very small change in resistance of the sensor at higher temperatures. Therefore, the $ZnSnO_3$ cubic crystallites operate as a sensing element to the $H_2$ only within a specific temperature window. The maximum gas response for 50 ppm $H_2$ is about 652.36 at 375 °C. Therefore, the temperature of 375 °C was chosen for further evaluating the $H_2$ sensing characteristics of the $ZnSnO_3$ cubic crystallites.

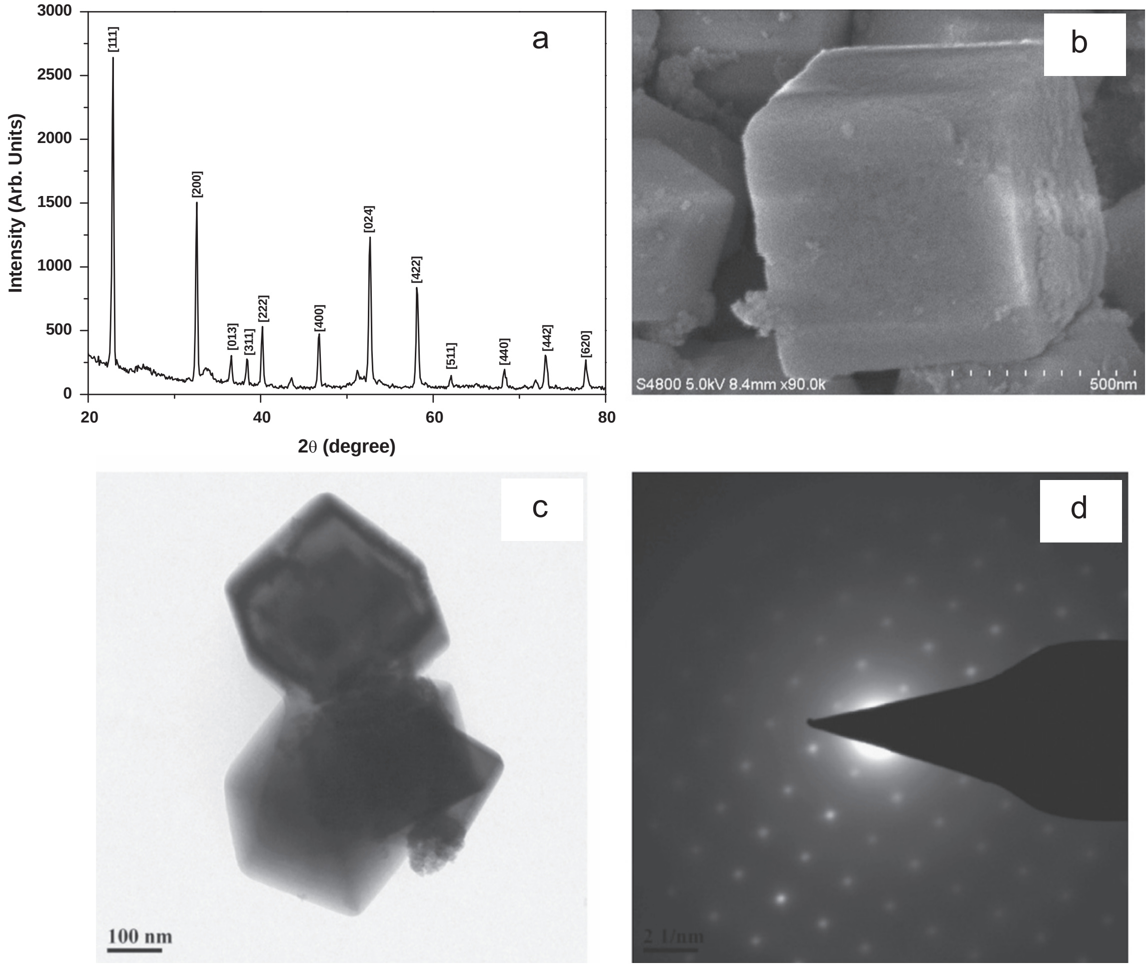


**Fig. 2.** (a) XRD pattern, (b) FESEM image, (c) TEM image and (d) the corresponding SAED pattern of as-synthesized $ZnSnO_3$ cubic crystallites.

Besides the gas response, the response and recovery times are also important parameters for a gas sensor. The response and recovery characteristics of the $ZnSnO_3$ cubic crystallites based sensor to 50 ppm $H_2$ at the optimum operating temperature of 375 °C is shown in Fig. 4(a). Five samples were tested from each batch and each sample was tested three times. It was observed that the resistance of the sensing element decreases upon injection of the $H_2$, which suggests that $ZnSnO_3$ cubic crystallites behave as a n-type semiconductor. From the curve, it can be seen that the sensor responded rapidly after introduction of $H_2$ and recovered immediately when it was exposed to air. For 50 ppm $H_2$, the sensor has response and recovery times of ~1 and 12 s, respectively.

The reproducibility of the $ZnSnO_3$ cubic crystallites based sensor was investigated by repeating the test three times. The representative dynamic gas response of the sensor upon periodic exposure to 50 ppm $H_2$ at the optimum operating temperature of 375 °C is shown in Fig. 4(b). The sensor showed good reproducibility and reversibility upon repeated exposure and removal of $H_2$ under same conditions. Furthermore, the repeated tests revealed that the gas response values are maintained and the recovery abilities are not reduced after several sensing cycles. Thus, the $ZnSnO_3$ cubic crystallites based sensor exhibits a stable and repeatable characteristic, which suggests that it can be used as a reusable sensing material for the detection of $H_2$.

The gas response of the sensor as a function of $H_2$ concentration at the optimum operating temperature of 375 °C is shown in Fig. 5. It is observed that the gas response increases continuously

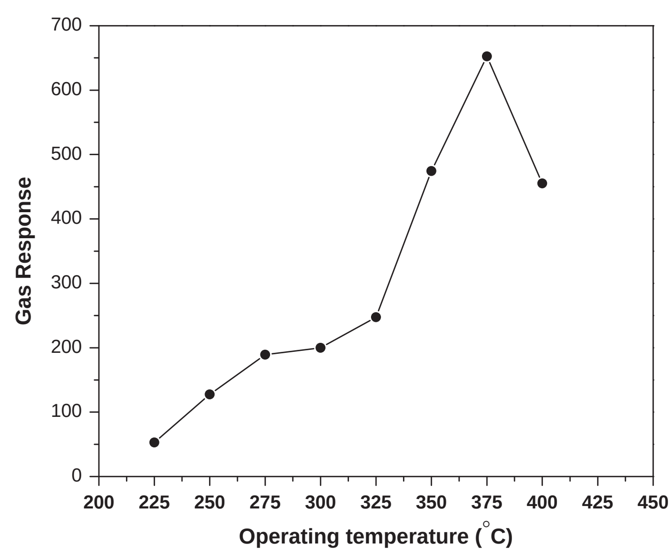


**Fig. 3.** Effect of operating temperature on the gas response of $ZnSnO_3$ cubic crystallites to 50 ppm $H_2$ gas.

with the increase in the $H_2$ concentration. According to previous reports [18,19], the gas response of the semiconductor oxide gas sensor can usually be empirically represented as:

$$\text{Gas response} = 1 + \alpha P_g{}^{\beta} \tag{2}$$

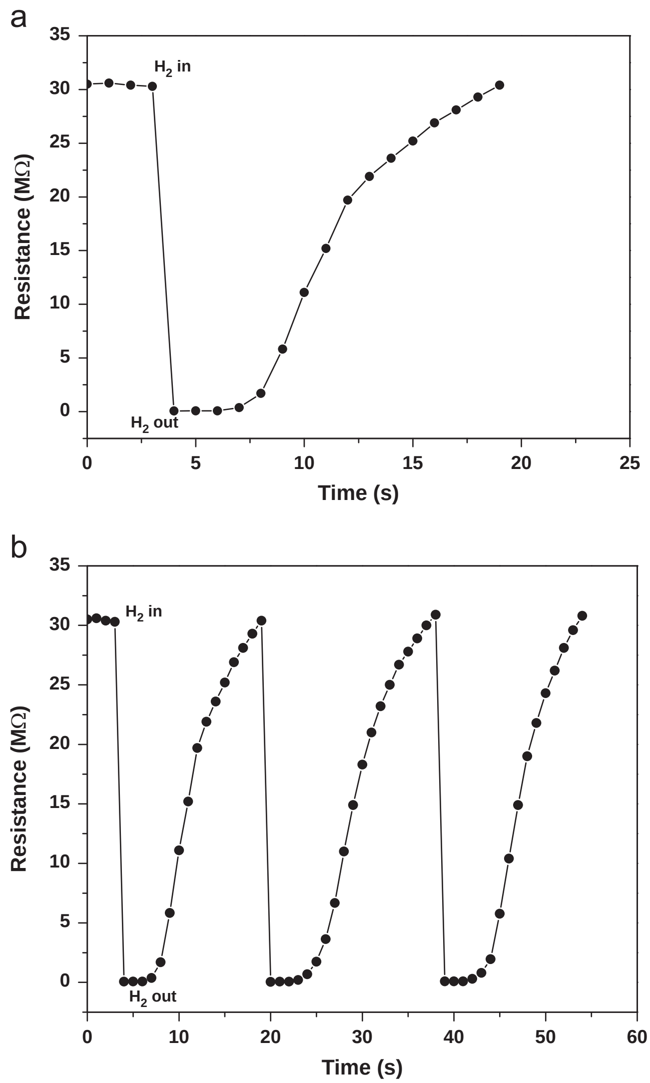


**Fig. 4.** (a) Response and recovery characteristics and (b) repetitive response of $ZnSnO_3$ cubic crystallites to 50 ppm $H_2$ gas at 375 °C.

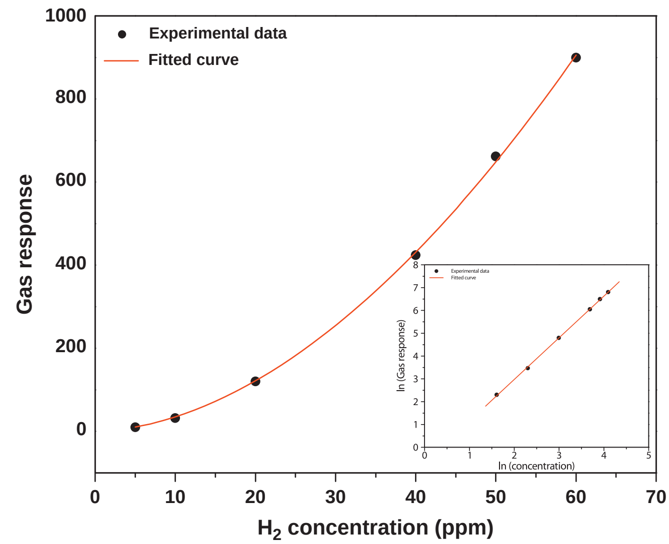


**Fig. 5.** Gas response of $ZnSnO_3$ cubic crystallites as a function of $H_2$ concentration at 375 °C. The inset shows the dilogarithm fit curve.

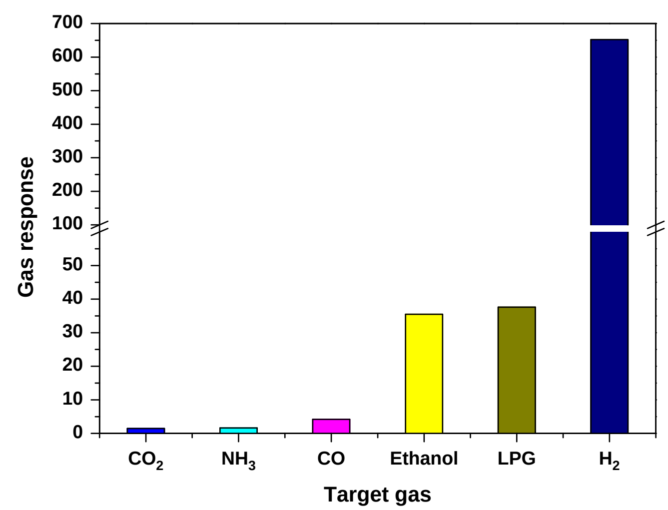


**Fig. 6.** Bar chart showing the gas response of $ZnSnO_3$ cubic crystallites for different gases. The gas concentration and operating temperature in all cases were 50 ppm and 375 °C, respectively.

where $\alpha$ is a concentration independent factor and $P_g$ is the target gas pressure that is directly proportional to its concentration ($C$). The exponent $\beta$ depends on the charge of the surface species, the stoichiometry of the elementary reactions on the surface and the size and morphology of the sensing material. In our case, the values of $\alpha$ and $\beta$ are found to be 0.496 and 1.834, respectively with $H_2$ concentration in the range of 5–60 ppm. The continuous curve shows the fit to the experimental data, illustrating clearly good quality of the fit. Thus, as shown in the inset of Fig. 5, the logarithm of gas response varies linearly with logarithm of $H_2$ concentration. The continuous curve shows a linear fit (ln(Gas response) $= -0.68 + 1.834\ \ln(C)$) to the experimental data with the correlation coefficient $R=0.99$. Hence, the $ZnSnO_3$ cubic crystallites based sensor can be reliably used to monitor the concentration of $H_2$ in the range 5–60 ppm.

The selectivity was also investigated by measuring the response of the $ZnSnO_3$ cubic crystallites based sensor to various gases including $H_2$, CO, $CO_2$, LPG, $NH_3$ and ethanol with a fixed concentration of 50 ppm at 375 °C. As shown in Fig. 6, the sensor exhibits highest response for $H_2$ ($S=652.36$) and low level response to $NH_3$ ($S=1.63$). In order to quantify the selectivity to $H_2$, the selectivity coefficient ($K$) was calculated further according to the definition [20]

$$K = \frac{S_{H_2}}{S_B} \tag{3}$$

where $S_{H_2}$ and $S_B$ are the responses of sensors in $H_2$ and B gas, respectively. The preferentially high response exhibited by the $ZnSnO_3$ cubic crystallites towards $H_2$ ($S=652.36$ to 50 ppm $H_2$ at 375 °C) compared to only 37.61 − 1.63 in case of other gases like LPG, $NH_3$, CO, $CO_2$ and ethanol is remarkable. The selectivity coefficient, $K$ for the $ZnSnO_3$ cubic crystallites varied in the order $CO_2 > NH_3 > CO >$ ethanol $>$ LPG. This means that the fabricated sensor based on $ZnSnO_3$ cubic crystallites could be used for the selective detection of $H_2$ when there is a mixture of $H_2$ and CO. All results suggest that the $ZnSnO_3$ cubic crystallites is a promising material for the fabrication of $H_2$ sensor.

### 3.4. Sensing mechanism

The most important features of the present investigation are—high gas response, rapid response-recovery, selectivity to $H_2$ against other gases, repeatability and relatively lower operating temperature. The observed sensing characteristics of the sensor are attributed to the crystal morphology of as-synthesized $ZnSnO_3$ cubic crystallites

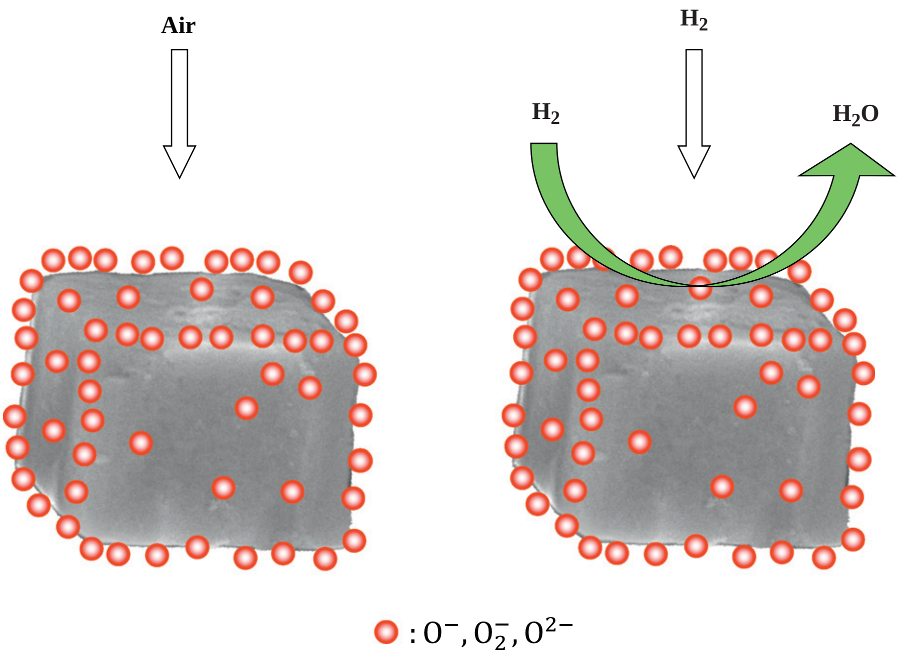


**Fig. 7.** Schematic diagram of $H_2$ sensing process of the $ZnSnO_3$ cubic crystallite.

that offers enhanced active sites for reaction of $H_2$ molecules with adsorbed oxygen. The gas sensing mechanism of semiconducting oxide gas sensors is a surface controlled process governed by adsorption and desorption of gas molecules, resulting the change in the resistance of the sensing material. The adsorption and desorption processes mainly depends on the surface morphology and orientation of the crystals. As the crystal size decreases, the ratio of edge to corner atoms increases. The edge and corner sites of the cubic crystallites of $ZnSnO_3$ exhibit lower adsorption enthalpies than terrace sites which serve as active sites for rapid adsorption of gas molecules [21].

The $ZnSnO_3$ is an n-type semiconductor, in which electrons are the majority carriers. By only considering a $ZnSnO_3$ cubic crystallite, the sensing process of $H_2$ gas is schematically depicted in Fig. 7. It is well known that oxygen is adsorbed on the surface of the $ZnSnO_3$ cubic crystallites as $O_2^-$, $O^-$or $O^{2-}$ ions by extracting the electrons from the conduction band [21,22]. The sensing mechanism is based on interaction between the negatively charged oxygen adsorbed on the surface of the $ZnSnO_3$ cubic crystallites and $H_2$ gas to be detected.

When $ZnSnO_3$ cubic crystallites are exposed to air, a certain amount of oxygen from air adsorb on its surface. The $ZnSnO_3$ cubic crystallites interact with the oxygen, by transferring the electrons from the conduction band to adsorbed oxygen atoms, resulting into the formation of ionic species such as $O_2^-$, $O^-$or $O^{2-}$. The reaction kinematics may be explained by the following reactions [21–23]

$$O_{2(gas)} \leftrightarrow O_{2(adsorbed)} \tag{4}$$

$$O_{2(adsorbed)} + e^- \leftrightarrow O^-_{2(adsorbed)} \tag{5}$$

$$O^-_{2(adsorbed)} + e^- \leftrightarrow 2O^-_{(adsorbed)} \tag{6}$$

$$O^-_{(adsorbed)} + e^- \leftrightarrow O^{2-}_{(lattice)} \tag{7}$$

The adsorbed oxygen species on $ZnSnO_3$ cubic crystallites act as electron acceptors that generate a surface depletion layer and thus, resistance of $ZnSnO_3$ cubic crystallites increases.

When such $ZnSnO_3$ cubic crystallites are exposed to a reducing gas like $H_2$, its atoms interact with these pre-adsorbed oxygen species and lattice oxygen and produce $H_2O$ molecules consuming oxygen from the surface of the $ZnSnO_3$ cubic crystallites. The reactions between ionic oxygen species and $H_2$ molecules can be represented by the following relations [24]

$$H_{2(gas)} \leftrightarrow H_{2(adsorbed)} \tag{8}$$

$$H_{2(adsorbed)} + O^-_{(adsorbed)} \rightarrow H_2O\ (g) + e^- \tag{9}$$

$$H_{2(adsorbed)} + O^{2-}_{(lattice)} \rightarrow H_2O\ (g) + 2e^- \tag{10}$$

The interaction of $H_2$ gas with the ionic oxygen species releases the electrons back to the conduction band of the $ZnSnO_3$ cubic crystallites. This contributes to the decrease in the depletion layer width and finally results in a decrease in the sensor resistance.

## 4. Conclusions

In summary, we reported for the first time a high performance $H_2$ sensor based on $ZnSnO_3$ cubic crystallites synthesized by a hydrothermal reaction. The hydrothermal conditions of 140 °C and 8 h ensure the formation of cubic crystallites with an average edge lengths of about 250–400 nm. The gas sensing measurements reveal that the sensor based on the $ZnSnO_3$ cubic crystallites exhibits higher gas response (~652.36 to 50 ppm $H_2$ gas at 375 °C), response time (~1 s), recovery time (~12 s), excellent repeatability, good selectivity and relatively lower operating temperature (~375 °C). This work demonstrates the potential of using $ZnSnO_3$ cubic crystallites as sensing material in the fabrication of $H_2$ sensors.

## Acknowledgment

The financial support from University Grants Commission (UGC), New Delhi, India through the SAP-DRS, Phase-II project no. F. 530/2/DRS/2010 (SAP-I) is gratefully acknowledged.

## References


[1] A. Gurlo, Nanoscale 3 (2011) 154–165.
[2] J. Zeng, M. Hu, W. Wang, H. Chen, Y. Qin, Sens. Actuators B 161 (2012) 447–452.
[3] E. Comini, Anal. Chim. Acta 568 (2006) 28–40.
[4] S. Agarwala, Z.H. Lim, E. Nicholson, G.W. Ho, Nanoscale 4 (2012) 194–205.
[5] D. Patil, P. Patil, V. Subramanian, P.A. Joy, H.S. Podar, Talanta 81 (2010) 37–43.
[6] R.B. Waghulade, R. Pasricha, P.P. Patil, Talanta 72 (2007) 594–599.
[7] D. Patil, V. Patil, P. Patil, Sens. Actuators B 152 (2011) 299–306.
[8] Y. Jia, L. He, Z. Guo, X. Chen, F. Meng, T. Luo, M. Li, J. Liu, J. Phys. Chem. C 113 (2009) 9581–9587.
[9] C. Li, D. Zhang, B. Lei, S. Han, X. Liu, C. Zhou, J. Phys. Chem. B 107 (2003) 12451–12455.
[10] X. Gou, G. Wang, J. Yang, J. Park, D. Wexler, J. Mater. Chem. 18 (2008) 965–969.
[11] C.C. Li, Z.F. Du, L.M. Li, H.C. Yu, Q. Wan, T.H. Wang, Appl. Phys. Lett. 91 (2007) 032101.
[12] J. Xu, X. Jia, X. Lou, J. Shen, Solid State Electron. 50 (2006) 504–507.
[13] X.Y. Xue, Y.J. Chen, Y.G. Wang, T.H. Wang, Appl. Phys. Lett. 86 (2005) 233101–233103.
[14] Y. Zeng, T. Zhang, H. Fan, W. Fu, G. Lu, Y. Sui, H. Yang, J. Phys. Chem. C 113 (2009) 19000–19004.
[15] Z. Wang, J. Liu, F. Wang, S. Chen, H. Luo, X. Yu, J. Phys. Chem. C 14 (2010) 13577–13582.
[16] H. Fan, Y. Zeng, X. Xu, N. Lv, T. Zhang, Sens. Actuators B 153 (2011) 170–175.
[17] S. Verhelst, R. Sierens, Int. J. Hydrogen Energy 26 (2001) 987–990.
[18] I.D. Kim, A. Rothschild, T. Hyodo, H.L. Tuller, Nano Lett. 6 (2006) 193–198.
[19] A. Yu, J. Qian, H. Pan, Y. Cui, M. Xu, L. Tu, Q. Chai, X. Zhou, Sens. Actuators B 158 (2011) 9–16.
[20] M. Siemons, U. Simon, Sens. Actuators B 126 (2007) 595–603.
[21] A. Sivapunniyam, N. Wiromrat, M.T.Z. Myint, J. Dutta, Sens. Actuators B 157 (2011) 232–239.
[22] H. Mbarek, M. Saadoun, B. Bessis, Mater. Sci. Eng. C 26 (2006) 500–504.
[23] K. Arshak, I. Gaidan, Sens. Actuators B 111 (2005) 58–62.
[24] O. Lupan, G. Chai, L. Chow, Microelectron. Eng. 85 (2008) 2220–2225.